Intensive Care Med (2000) 26: 1215–1227

ORIGINAL

L. Puybasset
P. Gusman
J.-C. Muller
P. Cluzel
P. Coriat
J.-J. Rouby
and the CT Scan ARDS Study Group

Regional distribution of gas and tissue in acute respiratory distress syndrome. III. Consequences for the effects of positive end-expiratory pressure

Received: 13 July 1999
Final revision received: 9 February 2000
Accepted: 10 April 2000

The following members of the CT Scan ARDS Study Group participated in this study: L. Gallart and M. Puig, Servei d'Anestesiologia, Hospital Universitari del Mar, Barcelona, Spain; G. S. Umamaheswara Rao, Department of Anesthesia, National Institute of Mental Health and Neurosciences, Bengalore, India; S. Vieira, Hospital Das Clinicas de Porto Allegre, UFRGS, Brazil; Q. Lu, M. O. Roussat, J.-D. Law-Koune, and L. Abdennour, Réanimation Chirurgicale Pierre Viars, Hôpital de La Pitié-Salpêtrière, Paris, France; J. Richecoeur, Réanimation médicale, Pontoise; D. Gava and F. Préteux, Institut National des télécommunications, Evry, France.

L. Puybasset (✉) · P. Gusman · J.-C. Muller
P. Cluzel · P. Coriat · J.-J. Rouby (✉)
Réanimation Chirurgicale Pierre Viars, Department of Anesthesiology, and the Department of Radiology, Hôpital de la Pitié-Salpêtrière, University of Paris Pierre et Marie Curie, 47–83 boulevard de l'Hôpital, 75013 Paris, France
e-mail: louis.puybasset@psl.ap-hop-paris.fr
jean-jacques.rouby@psl.ap-hop-paris.fr
Tel.: + 33-1-42177300
Fax: + 33-1-42177326

Present address:
P. Gusman
Department of Anesthesiology, UNESP, Botucatu, Brazil

Abstract *Objective*: To determine whether differences in lung morphology assessed by computed tomography (CT) affect the response to positive end-expiratory pressure (PEEP).
Design: Prospective study over a 53-month period.
Setting: Fourteen-bed surgical intensive care unit of a university hospital.
Patients and participants: Seventy-one consecutive patients with early adult respiratory distress syndrome (ARDS).
Measurements and results: Fast spiral thoracic CT was performed at zero end-expiratory pressure (ZEEP) and after implementation of PEEP 10 cmH_2O. Hemodynamic and respiratory parameters were measured in both conditions. PEEP-induced overdistension and alveolar recruitment were quantified by specifically designed software (Lungview). Overdistension occurred only in the upper lobes and was significantly correlated with the volume of lung, characterized by a CT attenuation ranging between –900 and –800 HU in ZEEP conditions. Cardiorespiratory effects of PEEP were similar in patients with primary and secondary ARDS. PEEP-induced alveolar recruitment of the lower lobes was significantly correlated with their lung volume (gas + tissue) at functional residual capacity. PEEP-induced alveolar recruitment was greater in the lower lobes with "inflammatory atelectasis" than in the lower lobes with "mechanical atelectasis." Lung morphology as assessed by CT markedly influenced the effects of PEEP: in patients with diffuse CT attenuations PEEP induced a marked alveolar recruitment without overdistension, whereas in patients with lobar CT attenuations PEEP induced a mild alveolar recruitment associated with overdistension of previously aerated lung areas. These results can be explained by the uneven distribution of regional compliance characterizing patients with lobar CT attenuations (compliant upper lobes and stiff lower lobes) contrasting with a more even distribution of regional compliances observed in patients with diffuse CT attenuations.
Conclusions: In patients with ARDS, the cardiorespiratory effects of PEEP are affected by lung morphology rather than by the cause of the lung injury (primary versus secondary ARDS). The regional distribution of the loss of aeration and the type of atelectasis – "mechanical" with a massive loss of lung volume, or "inflammatory" with a preservation of lung volume – characterizing the lower lobes are the main determinants of the cardiorespiratory effects of PEEP.

Key words Acute respiratory distress syndrome · Positive end-expiratory pressure · Computed tomography · Alveolar recruitment · Lung overdistension

Introduction

Positive end-expiratory pressure (PEEP) is considered as a critical means for reversing the refractory hypoxemia resulting from acute respiratory distress syndrome (ARDS). However, its optimal level is still the subject of controversy. PEEP-induced increase in PaO_2 is thought to result from alveolar recruitment, redistribution of extravascular lung water, and reduction in pulmonary blood flow through shunt units. In the 1980s Gattinoni et al. [1, 2] demonstrated that PEEP acts mainly as a counterforce opposing the pressure exerted by the edematous lung on the dependent bronchioles. As a consequence, PEEP appears more efficient at recruiting nondependent than dependent lung areas [2, 3]. It has also been shown that PEEP-induced alveolar recruitment is more efficient in cephalic than in caudal lung regions, likely because of a cephalocaudal gradient in the transpulmonary pressure [3]. More recently Gattinoni et al. [4] compared the effects of PEEP in patients with primary and secondary ARDS. The former were characterized by predominant alterations in lung compliance whereas the latter were characterized by predominant alterations in chest wall compliance. The lungs of patients with secondary ARDS were more prone to be recruited by PEEP than those of patients with primary ARDS.

We hypothesized that the effects of PEEP also depend upon lung morphology and compared the response to PEEP in the three groups of patients previously described in parts 1 [5] and 2 [6]. The analysis of the effects of PEEP was based on computed tomography (CT) since this method is the only one that allows clear distinction between PEEP-induced alveolar recruitment and PEEP-induced distension and overdistension [7].

Methods and materials

Patients

This prospective study included 71 consecutive patients with early ARDS and 11 healthy volunteers. Informed consent was obtained from the patients' next of kin. Clinical characteristics of the patients and the healthy volunteers have been extensively described in parts 1 [5] and 2 [6]. ARDS was considered primary in 49 patients (35 bronchopneumonias, 7 pulmonary contusions, 7 aspirations), secondary in 20 (4 extracorporeal circulations, 1 intra-abdominal sepsis, 15 extra-abdominal sepsis), and potentially both in two patients. Patients with primary ARDS were younger and more hypoxemic than those with secondary ARDS and had a pressure-volume curve that was significantly shifted to the right (Table 1, Fig. 1).

Lung morphology and cardiorespiratory parameters measured in zero end-expiratory pressure (ZEEP) were reported in parts 1 and 2 of the present study [5, 6]. All patients were sedated and paralyzed with fentanyl, midazolam, and vecuronium and were ventilated using controlled mechanical ventilation and FIO_2 of 1. All patients were monitored using a fiberoptic thermodilution pulmonary artery catheter and a radial or femoral arterial catheter.

Table 1 Cardiorespiratory parameters in patients with primary and secondary ARDS (PEEP = 0, FIO_2 100%); FRC and volume of lung tissue were obtained in 16 patients with primary ARDS and 32 patients with secondary ARDS (*Qs/Qt* pulmonary shunt, *MPAP* mean pulmonary arterial pressure, *PVRI* pulmonary vascular resistance index, *RAP* right atrial pressure, *MAP* mean arterial pressure, *SVRI* systemic vascular resistance index, *PCWP* pulmonary capillary wedge pressure, *CI* cardiac index, *FRC* functional residual capacity)

	Primary ARDS ($n = 49$)	Secondary ARDS ($n = 20$)
Age	53 ± 18	62 ± 13*
Survival rate (%)	45	55
PaO_2 (mm Hg)	85 ± 34	107 ± 48*
Qs/Qt (%)	48 ± 10	42 ± 11*
$PaCO_2$ (mm Hg)	46 ± 9	44 ± 8
FRC (ml)	1483 ± 690	1759 ± 744
Lung tissue (ml)	1650 ± 484	1658 ± 411
CI ($l\ min^{-1}\ m^{-2}$)	4.1 ± 1.7	3.3 ± 1.0
RAP (mm Hg)	8 ± 4	8 ± 4
PCWP (mm Hg)	9 ± 4	9 ± 4
SVRI (dyne $s^{-1}\ cm^{-5}\ m^2$)	1706 ± 780	1824 ± 591
MAP (mm Hg)	82 ± 16	77 ± 14
MPAP (mm Hg)	28 ± 9	26 ± 7
PVRI (dyne $s^{-1}\ cm^{-5}\ m^2$	439 ± 299	419 ± 169

*$p < 0.05$ vs. patients with primary ARDS

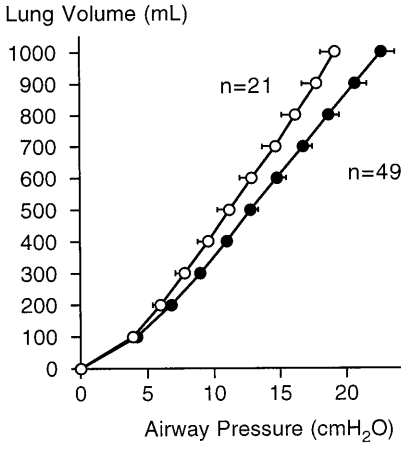

Fig. 1 Pressure-volume curves of the patients with primary (●) and secondary ARDS (○). The two curves are significantly different ($p < 0.001$)

Hemodynamic, respiratory, and lung volume changes induced by a PEEP of 10 cmH_2O were measured.

High-resolution and spiral thoracic CT

Acquisition of CT, classification of patients, and measurement of lung volumes

As described in detail in part 1 of the present study [5], lung scanning was performed from the apex to the diaphragm after an intravenous injection of 80 ml contrast medium in ZEEP and PEEP

10 cmH_2O. CT sections in PEEP were acquired at end-expiration after clamping the connecting piece between the Y piece and the endotracheal tube. Airway pressure was continuously monitored on a Propaq 104 EL monitor (Protocol System, North Chicago, Ill., USA) to ensure that a pressure of 10 cmH_2O was actually applied. Each patient's CT image was classified by an independent radiologist (P.C.) in one of the three groups according to definitions given in part 1 [5]: group 1, lobar attenuations; group 2, diffuse attenuations; group 3, patchy attenuations.

The volumes of gas and tissue were measured using a method previously described [7, 8, 9]. For each lung region of interest, the total volume, volume of gas and tissue, and fraction of gas were computed using equations provided in part 1 [5]. The overall lung volume (gas + tissue) at end-expiration was defined as end-expiratory lung volume. The volume of gas present in both lungs at end-expiration was defined as functional residual capacity (FRC).

Definition of PEEP-induced alveolar recruitment

PEEP-induced alveolar recruitment was computed on all CT sections according to Gattinoni et al. [8, 10]: alveolar recruitment (ml) = volume of nonaerated lung areas in ZEEP minus volume of nonaerated lung areas in PEEP. A positive value of this difference indicates alveolar recruitment and a negative value alveolar derecruitment. Nonaerated lung areas were defined as lung regions characterized by CT attenuation ranging between –100 and + 100 HU. PEEP-induced overdistension was measured as recommended by Vieira et al. [7]: overdistension (ml) = volume of overdistended lung areas in PEEP minus volume of overdistended lung areas in ZEEP.

Distribution of gas and tissue along the cephalocaudal and anteroposterior axes

In each condition the distribution of gas and tissue along the cephalocaudal axis was determined at end-expiration in the patients and healthy volunteers by taking into consideration each 10-mm-thick CT section between the apex and the lung base. The distribution of gas and tissue along the anteroposterior axis was determined on a single 10-mm-thick CT section located at the level of the tracheal carina. Ten contiguous compartments of similar height between the sternum and the vertebrae were taken into consideration as proposed by Gattinoni et al. [11]. A similar method was used to assess the distribution of PEEP-induced overdistension and alveolar recruitment along the cephalocaudal and the anteroposterior axes.

Calculation of regional respiratory compliances

The regional respiratory compliances of the upper and lower lobes were calculated as the changes in regional FRC (regional FRC at PEEP minus regional FRC at ZEEP) divided by 10 cmH_2O, the PEEP applied during the CT acquisition.

Hemodynamic and respiratory measurements

Within 12 h of the CT, hemodynamic and respiratory parameters were measured after a 1-h steady state in ZEEP and PEEP conditions. Throughout the study period methods used for measuring cardiorespiratory parameters were well defined, and measurements were performed according to standardized protocols that have been extensively described in part 2 of the present study [6]. Arterial and cardiac filling pressures, tracheal pressure, gas flow and tidal volume were simultaneously and continuously recorded on a Gould ES 1000 recorder. Cardiac output was measured using the intermittent O_2 semicontinuous thermodilution technique (CCO/SvO_2/VIP TD catheter, Baxter Healthcare, Irvine, Calif., USA). Hemoglobin and methemoglobin concentrations, and arterial and mixed venous oxygen saturations were measured using a calibrated OSM3 hemoximeter (Radiometer, Copenhagen, Denmark). Standard formulas were used to calculate cardiac index, pulmonary vascular resistance index, systemic vascular resistance index, right stroke work index, true pulmonary shunt (Qs/Qt), arteriovenous oxygen difference, oxygen delivery, oxygen extraction ratio, and oxygen consumption.

Statistical analysis

Comparisons between groups were performed by a two-way analysis of variance for one grouping factor (lobar, diffuse and patchy CT attenuations) and one repeated measure (ZEEP and PEEP). When the repeated measure or the interaction was significant, the effect of PEEP was tested in each group by a Student-Newman Keuls test for paired data. All data in the text and tables are presented as mean ± SD unless otherwise specified. The statistical analyses were performed using Statview 4.0.2 and SuperANOVA statistical software (Abacus Concepts, Berkeley, Calif., USA). The level of statistical significance was set at $p \leq 0.5$.

Results

Effects of PEEP on cardiorespiratory parameters

Overall

As shown on Tables 2 and 3, PEEP significantly increased PaO_2, arteriovenous oxygen difference, right atrial pressure, and pulmonary capillary wedge pressure and decreased Qs/Qt, $PaCO_2$, and cardiac index.

In the respective groups

The amplitude of the effects of PEEP on PaO_2 and Qs/Qt differed significantly between the three groups. As shown in Table 2, the effects of PEEP on PaO_2 and Qs/Qt were more pronounced in patients with diffuse CT attenuations than in patients with patchy CT attenuations than in patients with lobar CT attenuations (significant interactions). As shown in Table 3, in patients with lobar and patchy CT attenuations the cardiovascular parameters were not modified by PEEP, except for pulmonary capillary wedge pressure in patients with lobar and patchy CT attenuations.

Table 2 PEEP-induced changes (Δ) in respiratory parameters (FIO_2 100 %) in the three groups of patients (*LA* lobar *CT* attenuations, *DA* diffuse CT attenuations, *PA* patchy CT attenuations, SvO_2 mixed venous oxygen saturation, *Qs/Qt* pulmonary shunt, DO_2I oxygen delivery index, VO_2I oxygen consumption index, EaO_2 extraction ratio, $C\ (a\text{-}v)O_2$ arteriovenous oxygen difference)

	LA (n = 26)	DA (n = 16)	PA (n = 29)	PEEP	p Value[a]
ΔPaO_2 (mm Hg)	15 ± 38*	91 ± 71*	55 ± 60*	0.0001	0.0001
ΔHb (g dl^{-1})	0.0 ± 0.4	–0.1 ± 0.3	–0.1 ± 0.3	NS	NS
ΔPvO_2 (mm Hg)	–3 ± 6	4 ± 10	1 ± 4	NS	0.007
ΔSvO_2 (%)	–1 ± 4	5 ± 15	2 ± 6	NS	NS
ΔQs/Qt (%)	–5 ± 7*	–13 ± 6*	–7 ± 7*	0.001	0.003
ΔDO_2I (ml min^{-1} m^{-2})	–26 ± 40	–6 ± 103	–23 ± 80	0.03	NS
ΔVO_2I (ml min^{-1} m^{-2})	6 ± 15	–9 ± 30	–6 ± 23	NS	NS
ΔEaO_2 (%)	3 ± 4*	–3 ± 8	0 ± 4	NS	0.001
$\Delta C\ (a\text{-}v)O_2$ (vol/100ml)	0.4 ± 0.5*	0.1 ± 0. 6	0.1 ± 0.6	0.0001	NS
$\Delta PaCO_2$ (mm Hg)	–0.4 ± 4.7	–2.6 ± 2.7*	–1.3 ± 3.4*	0.003	NS

*$p < 0.05$ vs. ZEEP
[a]p values refer to the repeated measures ZEEP-PEEP (PEEP) and to the interaction between the 3 groups using a two-way analysis of variance

Table 3 PEEP-induced changes (Δ) in hemodynamic parameters (FIO_2 100 %) in the three groups of patients (*LA* lobar *CT* attenuations, *DA* diffuse *CT* attenuations, *PA* patchy *CT* attenuations, *MPAP* mean pulmonary arterial pressure, *PVRI* pulmonary vascular resistance index, *RAP* right atrial pressure, *RVSWI* right ventricular stroke work index, *MAP* mean arterial pressure, *SVRI* systemic vascular resistance index, *PCWP* pulmonary capillary wedge pressure, *HR* heart rate, *CI* cardiac index)

	LA (n = 26)	DA (n = 16)	PA (n = 29)	PEEP	p Value[a]
ΔMPAP (mm Hg)	1 ± 4*	0 ± 3	0 ± 4	NS	NS
ΔPVRI (dyne s^{-1} cm^{-5} m^2)	19 ± 102	17 ± 66	14 ± 99	NS	NS
ΔRAP (mm Hg)	1.0 ± 2.4*	0.7 ± 2.9	0.8 ± 2.6	0.003	NS
ΔRVSWI (g m^{-2})	0 ± 2	0 ± 3	0 ± 3	NS	NS
ΔMAP (mm Hg)	–2 ± 16	4 ± 12	–2 ± 9	NS	NS
ΔSVRI (dyne s^{-1} cm^{-5} m^2)	41 ± 598	224 ± 281	98 ± 325	0.047	NS
ΔPCWP (mm Hg)	1.8 ± 1.9*	0.4 ± 1.7	0.7 ± 1.7*	0.001	0.011
ΔHR (bpm)	1 ± 9*	–2 ± 7	–5 ± 10	NS	NS
ΔCl (l min^{-1} m^{-2})	–0.3 ± 0.3*	–0.5 ± 0.9*	–0.4 ± 0.8*	0.001	NS

*$p < 0.05$ vs. ZEEP
[a]p values refer to the repeated measures ZEEP-PEEP (PEEP) and to the interaction between the 3 groups using a two-way analysis of variance

Effects of PEEP on lung volumes

Overall

PEEP 10 cmH_2O increased FRC by 652 ± 298 ml. This increase was more pronounced in the upper than the lower lobes (491 ± 255 versus 161 ± 154 ml, $p < 0.001$). The total respiratory compliance of the upper lobes was greater than that of the lower lobes (49 ± 25 versus 16 ± 15 ml per cmH_2O, $p < 0.001$). When taking in consideration all patients, the volume of tissue did not change significantly after PEEP implementation. When considering individual data, the volume of tissue decreased in 42 % of the patients (mean change –118 ± 30 ml) and increased in the remaining 58 % (mean change + 95 ± 12 ml). The capillary wedge pressure and the right atrial pressure were higher in the group of patients in whom the volume of tissue decreased with PEEP than in those in whom the volume of tissue increased with PEEP (11 ± 4 mm Hg versus 8 ± 3 mm Hg and 9 ± 4 mm Hg versus 7 ± 3 mm Hg, $p = 0.01$). Otherwise, the two groups were similar for all the other parameters tested in ZEEP.

PEEP decreased the volume of nonaerated lung areas by 185 ± 179 ml. As a mean, the volume of poorly aerated areas did not change significantly after PEEP implementation. PEEP-induced alveolar recruitment was similar in the upper and lower lobes (104 ± 112 ml versus 81 ± 108 ml, NS). PEEP-induced alveolar recruitment in the lower lobes was significantly correlated with the end-expiratory lung volume according to the following equation:

Alveolar recruitment (ml) = 0.16 × end-expiratory lung volume (ml) – 24 ml
$r = 0.46$, $p = 0.0001$

Such a correlation was not observed in the upper lobes. Of the 96 individual lower lobes 31 (32 %) that were analyzed had “compression atelectasis,” characterized

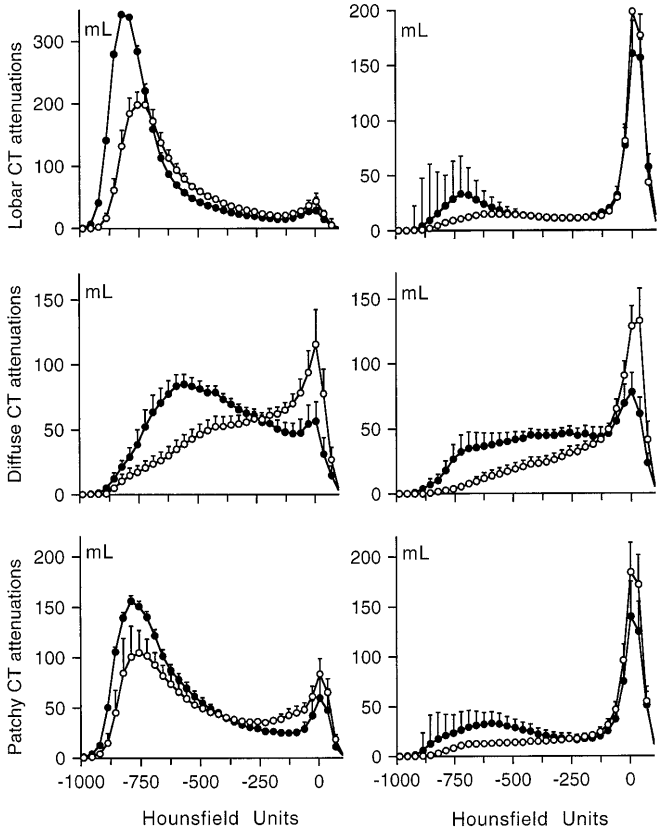

Fig. 2 Volumic distribution of CT attenuations in upper (*left*) and lower lobes (*right*) of patients with lobar CT attenuations (*upper*), diffuse CT attenuations (*middle*), and patchy CT attenuations (*lower*) at ZEEP (○) and PEEP 10 cmH_2O (●). Each value represented indicates the volume of six consecutive intervals of 5.47 HU. Data are mean ± SEM

by a dramatic reduction in FRC without any excess of lung tissue: FRC 28 ± 27 ml and volume of lung tissue 229 ± 40 ml in patients versus FRC 455 ± 153 ml and volume of lung tissue 241 ± 47 ml in healthy volunteers [5]. The remaining 65 lower lobes (68 %) had "inflammatory atelectasis," characterized by a dramatic reduction in FRC with a concomitant excess of lung tissue: FRC 93 ± 74 ml and volume of lung tissue 434 ± 136 ml. PEEP-induced alveolar recruitment was more pronounced in the lower lobes with "inflammatory atelectasis" than in the lower lobes with "compression atelectasis" (61 ± 67 ml versus 10 ± 53 ml, $p < 0.0001$).

In 26 patients (54 %), PEEP-induced alveolar recruitment was associated with PEEP-induced alveolar overdistension. Overdistension was observed exclusively in the upper lobes (37 ± 100 ml in the upper lobes versus 1 ± 5 ml in the lower lobes, $p < 0.05$). Overdistension was significantly correlated with the volume of lung parenchyma characterized by a CT attenuation ranging between –900 HU and –800 HU (parenchyma$_{-900;-800\ HU}$) in ZEEP conditions according to the following formula:

Volume of overdistension (ml) = 0.42 × parenchyma$_{-900;-800\ HU}$ (ml) – 18 ml
$r = 0.9$, $p = 0.0001$

This equation indicates that about 40 % of the lung characterized by a CT attenuation between –900 HU and –800 HU in ZEEP tends to be overdistended after implementation of a PEEP of 10 cmH_2O.

In the respective groups

Figure 2 depicts the volumic distribution of CT attenuations characterizing the upper and lower lobes of patients with lobar, diffuse, and patchy CT attenuations in ZEEP and PEEP conditions. Tables 4, 5, and 6 show the corresponding lung volumes. In ZEEP conditions the volumic distribution of CT attenuations in the upper lobes differed markedly between the three groups: unimodal with a peak located at –750 HU in patients with

Table 4 PEEP-induced changes (Δ) in lung volumes in the three groups of patients (*LA* lobar CT attenuations, *DA* diffuse CT attenuations, *PA* patchy CT attenuations, *ΔFRC* change in functional residual capacity)

	LA ($n = 26$)	DA ($n = 16$)	PA ($n = 29$)	PEEP	p Value[a]
ΔTotal volume (ml)	674 ± 303*	510 ± 281*	666 ± 355*	0.0001	NS
ΔPleural fluid (ml^{-1})	19 ± 53	46 ± 48	11 ± 76	0.01	NS
ΔFRC (ml)	696 ± 286*	507 ± 282*	634 ± 271*	0.0001	NS
ΔVolume of tissue (ml)	–22 ± 149	3 ± 107	32 ± 165	NS	NS
ΔOverdistended lung areas (ml)	47 ± 97*	2 ± 4	18 ± 24*	0.008	0.048
ΔNormally aerated lung areas (ml)	820 ± 344*	601 ± 473*	815 ± 354*	0.0001	NS
ΔPoorly aerated lung areas (ml)	–111 ± 169	290 ± 298	–6 ± 187	NS	0.0001
ΔNonaerated lung areas (ml)	–82 ± 68*	–383 ± 164*	–161 ± 151*	0.0001	0.0001

*$p < 0.05$ vs. ZEEP
[a] p values refer to the repeated measures ZEEP-PEEP (PEEP) and to the interaction between the 3 groups using a two-way analysis of variance

Table 5 PEEP-induced changes (Δ) in the volumes of the upper lobes in the three groups of patients (*LA* lobar CT attenuations, *DA* diffuse CT attenuations, *PA* patchy CT attenuations, *ΔFRC* change in functional residual capacity)

	LA ($n = 26$)	DA ($n = 16$)	PA ($n = 29$)	PEEP	p Value[a]
ΔTotal volume (ml)	573 ± 236*	258 ± 213*	467 ± 261*	0.0001	0.003
ΔFRC (ml)	594 ± 221*	284 ± 170*	465 ± 210*	0.001	0.0006
ΔVolume of tissue (ml)	–24 ± 155	–26 ± 102	2 ± 99	NS	NS
ΔOverdistended lung areas (ml)	46 ± 95*	1 ± 3	15 ± 23*	0.001	0.047
ΔNormally aerated lung areas (ml)	685 ± 201*	364 ± 281*	603 ± 276*	0.0001	0.004
ΔPoorly aerated lung areas (ml)	–114 ± 144*	103 ± 148*	–56 ± 142	NS	0.0006
ΔNonaerated lung areas (ml)	–45 ± 52*	–210 ± 127	–96 ± 94	0.0001	0.0001

*$p < 0.05$ vs. ZEEP
[a]p values refer to the repeated measures ZEEP-PEEP (PEEP) and to the interaction between the 3 groups using a two-way analysis of variance

Table 6 PEEP-induced changes (Δ) in the volumes of lower lobes in the three groups of patients (*LA* lobar CT attenuations, *DA* diffuse CT attenuations, *PA* patchy CT attenuations, *ΔFRC* change in functional residual capacity)

	LA ($n = 15$)	DA ($n = 14$)	PA ($n = 19$)	PEEP	p Value[a]
ΔTotal volume (ml)	100 ± 173*	252 ± 193*	199 ± 237*	0.0001	NS
ΔFRC (ml)	98 ± 153*	223 ± 159*	169 ± 149*	0.0001	NS
ΔVolume of tissue (ml)	2 ± 53	29 ± 108	30 ± 138	NS	NS
ΔOverdistended lung areas (ml)	1 ± 2	1 ± 2	2 ± 7	NS	NS
ΔNormally aerated lung areas (ml)	134 ± 226*	237 ± 251*	212 ± 182*	0.0001	NS
ΔPoorly aerated lung areas (ml)	3 ± 65	187 ± 191*	50 ± 107	0.0002	0.0001
ΔNonaerated lung areas (ml)	–37 ± 58	–174 ± 93*	–66 ± 122*	0.0001	0.001

*$p < 0.05$ vs. ZEEP
[a]p values refer to the repeated measures ZEEP-PEEP (PEEP) and to the interaction between the 3 groups using a two-way analysis of variance

lobar CT attenuations, unimodal with a peak located at 0 HU in patients with diffuse CT attenuations, and bimodal in patients with patchy CT attenuations. In contrast, the volumic distribution of CT attenuations in the lower lobes were nearly similar in the three groups of patients, the only difference being the volume of poorly aerated lung areas, which was greater in patients with diffuse CT attenuations than in patients with lobar and patchy CT attenuations.

As shown in Fig. 3, in both the upper and lower lobes PEEP-induced alveolar recruitment was the greatest in patients with diffuse CT attenuations, lowest in patients with lobar CT attenuations, and intermediate in patients with patchy CT attenuations. In contrast, PEEP-induced alveolar overdistension, which was observed only in the upper lobes, was the greatest in patients with lobar CT attenuations, intermediate in patients with patchy CT attenuations, and absent in patients with diffuse CT attenuations. In patients with lobar and patchy CT attenuations, overdistension predominated in nondependent lung regions.

Cephalocaudal and anteroposterior gradients of PEEP-induced overdistension and alveolar recruitment

Overall

Figure 4 shows the anteroposterior measured at the level of the carina and cephalocaudal distributions of gas and tissue, in ZEEP conditions for the patients and the healthy volunteers. The intrapulmonary gas and the lung tissue had a cephalocaudal distribution corresponding to the anatomical shape of the thorax. The sharp decline in gas and tissue after the 18th cm was due to the presence of the diaphragmatic cupola. In the healthy volunteers lung tissue and intrapulmonary gas were nearly homogeneously distributed within the lungs along the anteroposterior axis. In the patients the excess of lung tissue – assessed for a given lung level as the difference between the volume of lung tissue in patients minus the normal value of tissue measured in healthy volunteers – increased along the anteroposterior axis. The loss of gas – assessed for a given lung level as the difference between the volume of gas measured in healthy volunteers minus the volume of gas measured in patients – increased along the anteroposterior axis. Be-

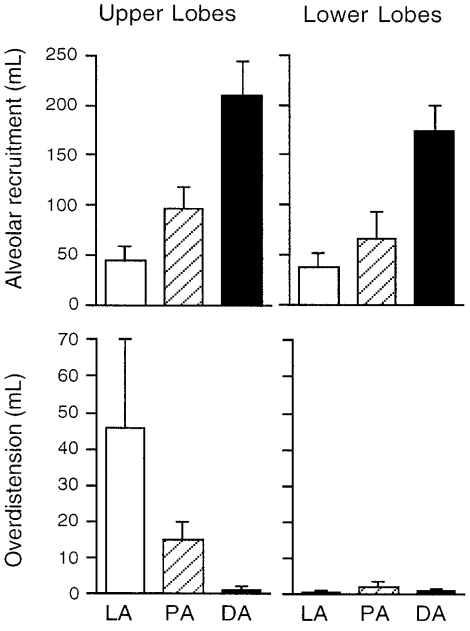

Fig. 3 Alveolar recruitment (*upper*) and overdistension (*lower*) induced by PEEP 10 cmH_2O in patients with lobar CT *attenuations (white bars*, *LA*), patchy CT attenuations (*hatched bars*, *PA*) and diffuse CT attenuations (*black bars*, *DA*) in upper (*left*) and lower (*right*) lobes analyzed separately. In upper and lower lobes recruitment was significantly different between the three groups. PEEP-induced overdistension was significantly different between the three groups in the upper lobes and was absent in lower lobes. Data are mean ± SEM

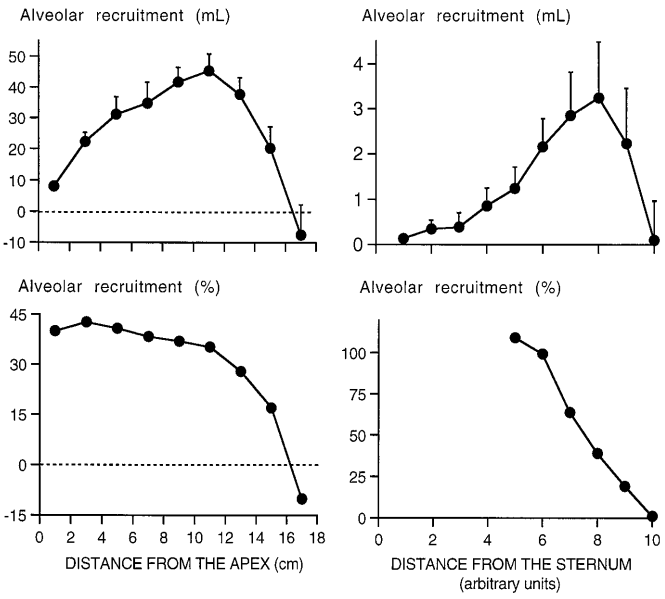

Fig. 5 Regional distribution of PEEP-induced alveolar recruitment expressed both in absolute values (*upper*) and percentage of variation (*lower*) in the cephalocaudal (*left*) and anteroposterior axes (*right*) computed in 48 patients with ARDS. *Dashed line* Threshold of alveolar derecruitment which was observed in the most caudal regions of the lung; *X-axis* The distance either from the apex (cm) or from the sternum. In this latter case each unit is the tenth of the total distance between the sternum and the vertebra

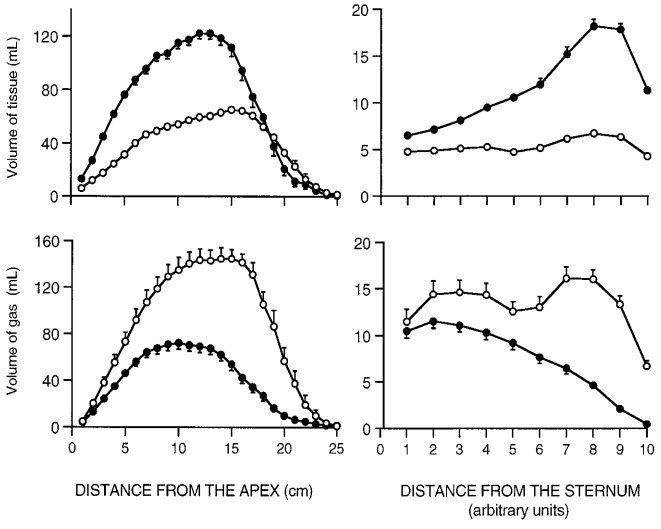

Fig. 4 Cephalocaudal (*left*) and anteroposterior (*right*) distribution of lung tissue (*upper*) and gas (*lower*) in the patients (●) and the healthy volunteers (○) assessed in ZEEP conditions. *X-axis* The distance either from the apex (cm) or from the sternum. In this latter case, each unit is the tenth of the total distance between the sternum and the vertebra

cause of the anatomical shape of the thorax and the reduction in the lung's cephalocaudal dimension observed in ARDS (see part 1 [5]) the distribution of the lung tissue in excess and loss of aeration along the cephalocaudal axis were more difficult to assess. Lung tissue in excess increased up to the 13th cm and then decreased in the caudal regions. The loss of gas was observed at all levels of the cephalocaudal axis.

As shown in Fig. 5, PEEP-induced alveolar recruitment expressed in absolute values was more pronounced in dependent and cephalic parts of the lungs. However, expressed as a percentage, alveolar recruitment was more pronounced in nondependent and cephalic lung areas than in dependent and caudal lung areas. As shown in Fig. 6, PEEP-induced overdistension, expressed in absolute values, predominated in caudal and nondependent lung areas. This distribution was similar to the one of the parenchyma of the healthy volunteers characterized by a CT attenuation between –900 and –800 HU at end-expiration.

In the respective groups

Figure 7 shows the anteroposterior distribution of gas and lung tissue in ZEEP conditions for the three groups

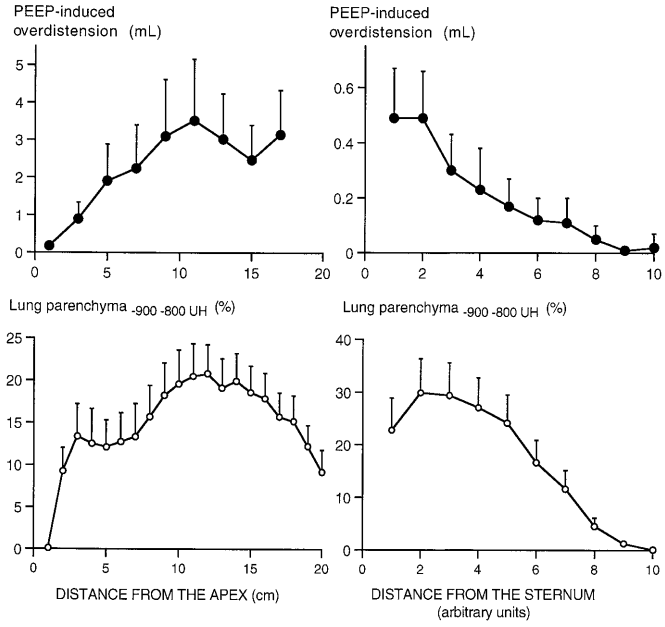

Fig. 6 Regional distribution of PEEP-induced alveolar overdistension in the cephalocaudal (*left*) and anteroposterior axes (*right*) computed on the 48 patients with ARDS (*upper*, *filled circles*, data expressed in absolute values) and proportion of "distended" lung parenchyma characterized by CT values between –900 and –800 HU (lung parenchyma$_{-900;-800\ HU}$) computed at FRC in the 11 healthy volunteers (*lower*, *filled circles*, data expressed in percentage of the overall volume). *X-axis* The distance either from the apex (cm) or from the sternum. In this latter case each unit is the tenth of the total distance between the sternum and the vertebra

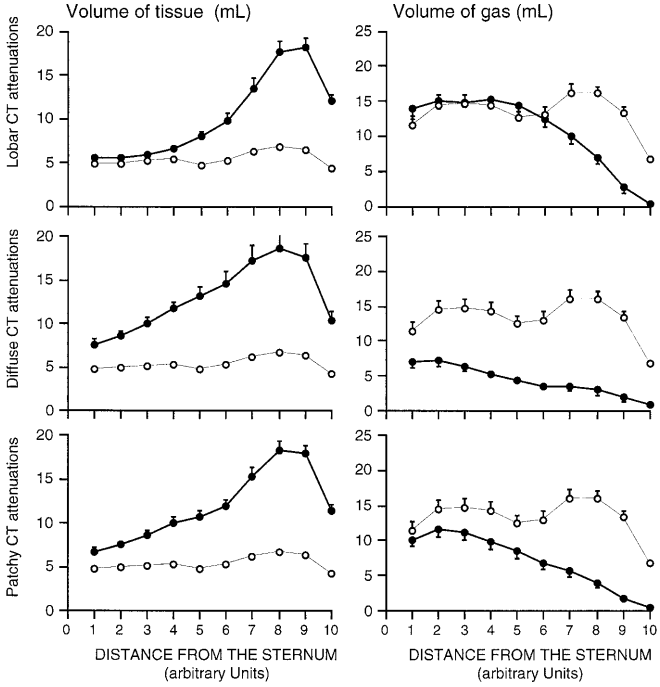

Fig. 7 Anteroposterior distribution of tissue (*left*) and gas (*right*) in patients with lobar CT attenuations (*upper*), diffuse CT attenuations (*middle*), patchy CT attenuations (*lower*) in ZEEP conditions. *X-axis* The distance from the anterior chest wall. Each unit is one-tenth of the total distance between the anterior chest wall and the vertebra (arbitrary units). *Open circles* Healthy volunteers; *filled circles* patients with ARDS

of patients as compared to the healthy volunteers. The excess of tissue – assessed for a given lung level as the difference between the volume of lung tissue measured in patients minus the normal value of lung tissue measured in healthy volunteers – increased along the anteroposterior axis in the three groups of patients. No excess of lung tissue was observed in the nondependent lung areas of patients with lobar CT attenuations. Figure 8 shows the cephalocaudal distribution of intrapulmonary gas and lung tissue in ZEEP conditions for the three groups of patients and for the healthy volunteers. In the three groups the excess of lung tissue increased along the cephalocaudal axis up to the 13–15th cm and then rapidly decreased.

The loss of aeration – assessed for a given lung level as the difference between the FRC measured in healthy volunteers minus the FRC measured in patients – increased along the anteroposterior and cephalocaudal axes in all groups (Figs. 7, 8). No loss of gas was observed in the most anterior and cephalic regions of patients with lobar CT attenuations in contrast to patients with diffuse CT attenuations in whom the loss of aeration was uniformly distributed.

As shown in Fig. 9, the percentage of alveolar recruitment decreased along the cephalocaudal axis (between the first and the 15th cm) in patients with lobar or patchy CT attenuations, but it remained constant in patients with diffuse CT attenuations. In patients with lobar and patchy CT attenuations, a PEEP-induced alveolar derecruitment was observed in the most caudal lung regions. The three groups of patients behave similarly regarding the distribution of PEEP-induced alveolar recruitment along the anteroposterior axis (data not shown).

Respiratory compliances of the upper and lower lobes in the three groups

Figure 10 shows the respiratory compliances of the upper and lower lobes for the three groups of patients. The respiratory compliance of the lower lobes was not significantly different between groups. In contrast, the respiratory compliance of the upper lobes was the greatest in patients with lobar CT attenuations, intermediate in patients with patchy attenuations and the lowest in patients with diffuse CT attenuations. The respiratory

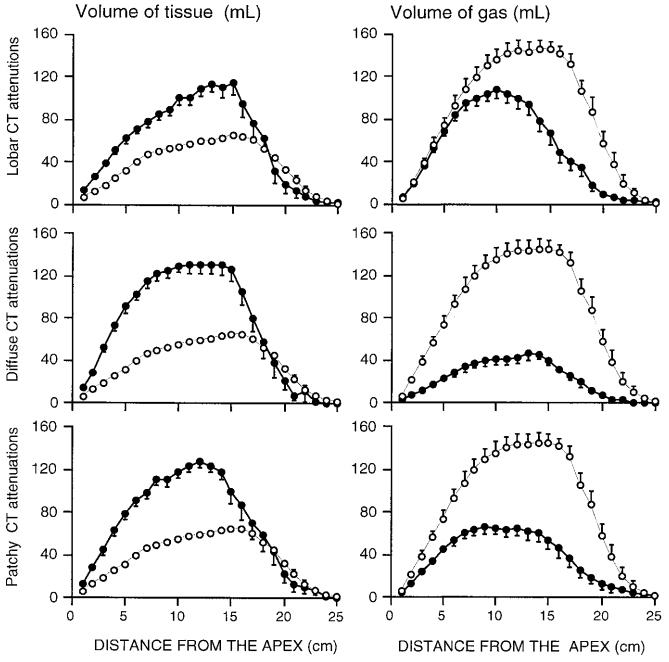

Fig. 8 Cephalocaudal gradient of tissue (*left*) and gas (*right*) in the three groups of patients in ZEEP conditions: lobar CT attenuations (*upper*), diffuse CT attenuations (*middle*), patchy CT attenuations (*lower*). *X-axis* The distance from the apex (in cm). *Open circles* Healthy volunteers; *filled circles* patients with ARDS

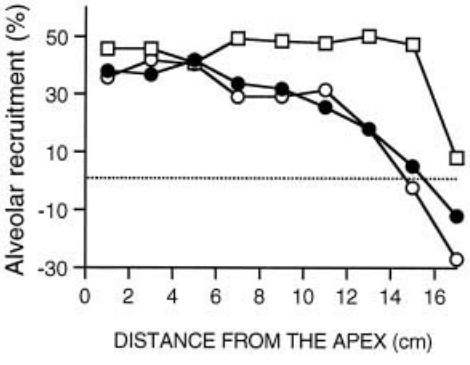

Fig. 9 Regional distribution of PEEP-induced alveolar recruitment expressed in percentage of variation along the cephalocaudal axis for the three groups of patients: patients with lobar CT attenuations (○), diffuse CT attenuations (□), patchy CT attenuations (●). *Dashed line* Threshold of PEEP-induced alveolar derecruitment. Values below this threshold indicate alveolar derecruitment.

compliances of the upper and lower lobes of patients with diffuse CT attenuations did not differ significantly. In patients with lobar and patchy CT attenuations the respiratory compliance of the upper lobes was significantly higher than the respiratory compliance of the lower lobes.

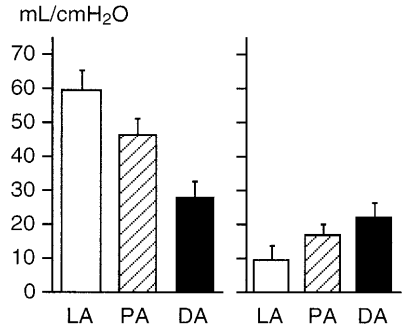

Fig. 10 Total respiratory compliance of the upper (left panel) and lower (right panel) lobes computed as the ratio between the PEEP-induced change in the volume of gas divided by a pressure of 10 cmH_2O (the PEEP value) in patients with lobar CT attenuations (*white bars*, *LA*), patchy CT attenuations (*hatched bars*, *PA*), and diffuse CT attenuations (*black bars*, *DA*). Data are mean ± SEM

Effects of PEEP in patients with primary and secondary ARDS

As shown in Table 7, the cardiorespiratory effects of PEEP were similar in patients with primary and secondary ARDS.

Discussion

This study demonstrates that the regional distribution of intrapulmonary gas and lung tissue in ARDS influences to a large extent the effects of PEEP: a maximum alveolar recruitment without evidence of overdistension is observed in patients with diffuse CT attenuations. In contrast, the administration of PEEP to patients with lobar CT attenuations is associated with a mild alveolar recruitment while some parts of the previously aerated lung regions are simultaneously overdistended. This result is likely related to a phenomenon of "lobar interdependence": in patients with lobar CT attenuation PEEP preferentially distends compliant upper lobes without recruiting atelectatic lower lobes; in patients with diffuse CT attenuations PEEP is evenly distributed within the lungs allowing an homogeneous alveolar recruitment of poorly compliant upper and lower lobes.

Measurements of PEEP-induced alveolar recruitment and lung overdistension

The density threshold used for determining lung overdistension was based on a previous work performed in healthy volunteers and comparing the volumic distribution of CT attenuations at FRC and at total lung capacity during a Valsalva maneuver [7]. The CT attenuation threshold characterizing lung overdistension was deter-

Table 7 Cardiorespiratory effects of PEEP in patients with primary and secondary ARDS (FIO_2 100%); the parameters derived from the Lungview analysis were obtained in 16 patients with primary ARDS and 32 patients with secondary ARDS (*ΔQs/Qt* change in pulmonary shunt, *ΔMPAP* change in mean pulmonary arterial pressure, *ΔPVRI* change in pulmonary vascular resistance index, *ΔRAP* change in right atrial pressure, *ΔMAP* change in mean arterial pressure, *ΔSVRI* change in systemic vascular resistance index, *ΔPCWP* change in pulmonary capillary wedge pressure, *ΔCI* change in cardiac index, *ΔFRC* change in functional residual capacity)

	Primary ARDS (n = 49)	Secondary ARDS (n = 20)
Respiratory effects		
ΔPaO2 (mm Hg)	54 ± 64	35 ± 58
ΔQs/Qt (%)	–8 ± 8	–6 ± 6
$\Delta PaCO_2$ (mm Hg)	–1.7 ± 3.4	–0.3 ± 4.7
Alveolar recruitment (ml)	148 ± 165	225 ± 180
Lung overdistension (ml)	42 ± 91	39 ± 113
ΔFRC (ml)	717 ± 312	600 ± 291
ΔLung tissue (ml)	32 ± 105	–9 ± 157
Cardiovascular effects		
ΔCI (l min^{-1} m^{-2})	–0.4 ± 0.8	–0.3 ± 0.4
ΔRAP (mm Hg)	1 ± 3	1 ± 2
ΔPCWP (mm Hg)	1 ± 2	1 ± 2
ΔSVRI (dyne s^{-1} cm^{-5} m^2)	43 ± 385	254 ± 525
ΔMAP (mm Hg)	–2 ± 12	3 ± 14
ΔMPAP (mm Hg)	1 ± 3	0 ± 4
ΔPVRI (dyne s^{-1} cm^{-5} m^2)	17 ± 91	17 ± 99

mined at –900 HU since more than 99% of healthy volunteers' lung parenchyma was characterized by CT values greater than –900 HU at FRC while 30% of the lung parenchyma was characterized by CT values ranging between –1000 and –900 HU at total lung capacity. This threshold is in accordance with that reported in previous studies performed in patients with emphysema showing that the volume of the lung characterized by CT values below –900 HU is well correlated with alteration in pulmonary function tests and degree of histological distension [12, 13, 14, 15]. However, at least theoretically, such a method might underestimate overdistension. Indeed, the spatial resolution of CT is rather low since a voxel contains between 2000 and 3000 alveoli. Therefore one cannot exclude that a voxel having a CT attenuation above –900 HU contains overdistended alveoli in a proportion that could be insufficient to reduce its radiological density below –900 HU. On the other hand, in the present study CT attenuations below –900 HU were observed in patients with lobar CT attenuations for a PEEP value as low as 10 cmH_2O, suggesting that this threshold is rather sensitive for detecting overdistension in clinical practice.

Gattinoni et al. defined PEEP-induced alveolar recruitment as the decrease in the volume of nonaerated lung areas characterized by a CT attenuation greater than –100 HU [8, 10]. The major advantages of this definition are its simplicity and ease of use since the calculation of alveolar recruitment does not require any regional analysis. However, this method has the disadvantage of ignoring the reaeration of previously poorly aerated lung areas characterized by a CT attenuation ranging between –500 HU and –100 HU. In the present study it is likely that this potential flaw had limited consequences on assessment of PEEP-induced alveolar recruitment since, as a mean, the volume of poorly aerated lung areas did not change significantly with PEEP.

PEEP-induced alveolar recruitment

There is a general agreement for defining PEEP-induced alveolar recruitment as the reopening of previously collapsed bronchioles. As a consequence, the volume of nonaerated lung decreases and FRC increases. In contrast, there is still a controversy as to whether PEEP-induced alveolar recruitment is associated with a reduction in extravascular lung water. Some experimental data suggest that PEEP decreases the amount of alveolar edema [16, 17, 18] while others report no change or an increase in extravascular lung water [19, 20]. In the present study PEEP increased the volume of lung tissue in 58% of the patients and decreased the volume of tissue in the remaining 42%. The existence of a greater capillary wedge pressure in the latter suggests that the main determinant of the effect of PEEP on extravascular lung water is the microvascular pressure, thus explaining the conflicting results found in different models of acute lung injury.

In the lower lobes PEEP-induced alveolar recruitment was inversely related to the end-expiratory lung volume in ZEEP conditions. This result is in accordance with the data obtained in a more limited series of patients [3]. When the loss of aeration was not associated with an increase in lung tissue, the end-expiratory volume of the lower lobes was dramatically reduced, and a PEEP of 10 cmH_2O was unable to induce alveolar recruitment. Such a feature is highly reminiscent of pure "compression atelectasis," a condition in which the opening pressure of the lung is above 30 cmH_2O [21]. In contrast, when the loss of aeration was associated with an excess in lung tissue, end-expiratory volume of the lower lobes was relatively preserved, and moderate levels of PEEP were able to recruit the collapsed lung. Such a feature is highly reminiscent of "inflammatory atelectasis," a condition in which collapse of dependent bronchioles is essentially depending upon the ventrodorsal gradient of pressure related to the increased lung weight. Since the anteroposterior diameter of the thorax is less than 15 cm in the majority of the patients, it is not surprising that even moderate PEEP levels are effective for reopening dependent bronchioles by reversing this gravitational pressure gradient [1]. Al-

though always observed in cephalic and nondependent lung regions, PEEP-induced alveolar recruitment is variable from one patient to another, depending on the respective importance of each mechanism.

PEEP-induced overdistension

Another important result of the present study is that in 54% of the patients with ARDS PEEP-induced alveolar recruitment occurred together with overdistension of previously well-aerated lung regions. A similar result has been reported recently in a more limited series of patients [9]. The volume of overdistension was linearly correlated with the volume of lung having a CT attenuation ranging between –900 and –800 HU in ZEEP conditions. Such lung areas, which can be considered as already "distended" in the absence of PEEP, are normally present in the nondependent lung regions and represent 17% of the overall lung parenchyma of healthy volunteers (Fig. 6). Because of the dramatic loss of aeration characterizing the lower lobes in ZEEP conditions, lung regions characterized by a CT value between –900 and –800 HU are absent in the dependent and caudal parts of the lungs of patients with ARDS. However, in a few patients, these areas were still found in nondependent parts of the upper lobes in ZEEP conditions, explaining why PEEP-induced overdistension was observed in cephalic parts of the lungs.

Cardiorespiratory effects of PEEP according to differences in lung morphology

For a PEEP level of 10 cmH_2O, alveolar recruitment was much lower in patients with lobar CT attenuations than in patients with diffuse CT attenuations in whom the reaeration of the lung was homogeneous, involving both upper and lower lobes. In patients with lobar CT attenuations, the first effect of PEEP was to increase the amount of gas present in the upper lobes that were already aerated in ZEEP conditions, resulting in regional lung overdistension. The lungs of these patients can be assimilated to a bicompartmental model composed of a compliant and a stiff compartment (upper and lower lobes). These compartments interact one with the other in response to PEEP in such a way that the distension of one prevents the recruitment of the other. On the other hand, in patients with diffuse CT attenuations, the primary effect of PEEP was to increase the amount of gas in both upper and lower lobes that were characterized by a dramatic loss of aeration. The lung of patients with diffuse CT attenuations can be assimilated to a monocompartmental model since the upper and lower lobes are characterized by similar alterations in lung mechanics. As a consequence, any increase in end-expiratory pressure is homogeneously distributed within the lung and results in an homogeneous reopening of collapsed distal bronchioles. Homogeneous lungs in terms of loss of aeration, as observed in patients with diffuse CT attenuations, are more prone to be recruited by PEEP whereas inhomogeneous lungs, as observed in patients with lobar CT attenuations, are more prone to be overdistended by PEEP. Although not tested in the present study to avoid excessive X-ray exposure, it is highly likely that the phenomenon of "lobar interdependence" is even more accentuated at end-inspiration for a given PEEP level.

Theoretically, hemodynamic effects of PEEP should be influenced by the absence or the presence of PEEP-induced overdistension. Mechanical compression of pulmonary and extrapulmonary vessels should result in an increase in pulmonary vascular resistance and a decrease in cardiac index. In fact, PEEP did increase the arteriovenous oxygen difference, the extraction ratio of oxygen, and the cardiac filling pressures only in patients with lobar CT attenuations in whom some degree of PEEP-induced overdistension could be observed.

Cardiorespiratory effects of PEEP in primary and secondary ARDS

Recently, Gattinoni et al. [4] studied the effects of PEEP in 12 patients with primary ARDS and 9 patients with secondary ARDS. Patients with primary ARDS had a lower lung compliance and a greater chest wall compliance than patients with secondary ARDS and PEEP induced a significant alveolar recruitment only in patients with secondary ARDS. The authors hypothesized that lung consolidation was predominant in patients with primary ARDS preventing any possibility of alveolar recruitment whereas interstitial edema was predominant in patients with secondary ARDS allowing the reopening of collapsed bronchioles. The data of the present study do not support this view. No difference was found as far as cardiorespiratory effects of PEEP between patients with primary and secondary ARDS. PEEP-induced alveolar recruitment and overdistension were not affected by the cause of ARDS. It is likely that the discrepancies between the two studies result from differences in the methods used for assessing PEEP-induced alveolar recruitment.

A direct CT approach was used in the present study whereas an indirect approach was used by Gattinoni et al. [4]. These authors estimated PEEP-induced alveolar recruitment by a method derived from the analysis of the pressure-volume curves in ZEEP and PEEP proposed by Ranieri et al. [22]. Alveolar recruitment is defined as the difference between the end-expiratory lung

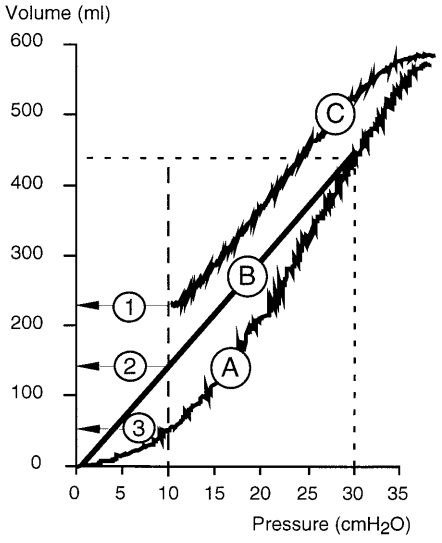

Fig. 11 The figure shows the calculation of PEEP-induced alveolar recruitment according to the method developed by Ranieri et al. [22] in two conditions: *1* the pressure-volume curve in ZEEP is actually measured and is characterized by a marked lower inflection point (*P-V curve A*); *2* the pressure-volume curve in ZEEP conditions is derived from the measurement of the quasistatic compliance (*P-V curve B*, *oblique line*). The plateau pressure measured in ZEEP conditions for a tidal volume of 430 ml is 30 cmH_2O. The quasistatic compliance is 14 ml/cmH_2O. The slope of the P-V curve is 23 ml/cmH_2O. The change in end-expiratory lung volume measured after the release of PEEP 10 cmH_2O is 220 ml (*horizontal arrow 1*). *Curve C* The pressure-volume curve measured in PEEP 10 cmH_2O. If the actual P-V curve measured in ZEEP is taken into consideration (*curve A*), the computed alveolar recruitment is 165 ml (lung volume indicated by the *horizontal arrow 1* minus lung volume, indicated by the *horizontal arrow 3*). If the derived P-V curve is taken into consideration (*curve B*), the computed recruitment is 85 ml (lung volume indicated by the *horizontal arrow 1* minus lung volume indicated by the *horizontal arrow 2*). In this particular patient, alveolar recruitment is underestimated by 48 % in the second condition

volume directly measured by releasing PEEP minus the lung volume corresponding to the same airway pressure indirectly measured from the pressure volume curve performed in ZEEP conditions. However, in the Gattinoni et al. study pressure-volume curves were not actually measured but derived from the respiratory compliance obtained by dividing the tidal volume by the inspiratory plateau pressure. As a consequence, Gattinoni et al. did not take into account a possible lower inflection point in their calculation of the lung volume corresponding to the PEEP level. As shown in Fig. 11, their method of calculating alveolar recruitment tends to underestimate PEEP-induced alveolar recruitment when a lower inflection point is present. According to Fig. 1, this bias concerns predominantly patients with primary ARDS. Very likely the lack of measurement of the pressure-volume curve in ZEEP conditions resulted in an underestimation of PEEP-induced alveolar recruitment in patients with primary ARDS.

Clinical implications

In parts 1 [5] and 2 [6] of the present study we demonstrate that differences in CT patterns correspond to differences in lung volumes, chest radiography, cause, mortality rate, and lung mechanics. As shown in the present study, the cardiorespiratory effects of PEEP are affected by lung morphology rather than by the cause of ARDS. PEEP is poorly efficient in patients with lobar CT attenuations and often associated with overdistension of previously aerated lung areas, particularly when a major reduction in the end-expiratory lung volume of the lower lobes is present ("compression atelectasis"). In this group of patients alternative strategies such as prone or upright positions appear attractive. In contrast, patients with diffuse CT attenuations demonstrate a marked alveolar recruitment with PEEP without any evidence of overdistension. As a consequence, the rationale for choosing ventilatory settings is to increase mean airway pressure, all the more since PEEP-induced alveolar recruitment starts from the lower inflection point and continues along the linear part of the pressure volume curve [9, 23]. If such a strategy is chosen, the plateau airway pressure should be maintained below the upper distending pressure measured on the pressure volume curve by reducing tidal volume in order to prevent mechanical ventilation-induced lung barotrauma [24].

References

1. Gattinoni L, D'andrea L, Pelosi P, Vitale G, Pesenti A, Fumagalli R (1993) Regional effects and mechanism of positive end-expiratory pressure in early adult respiratory distress syndrome. JAMA 269: 2122–2127

2. Gattinoni L, Pelosi P, Crotti S, Valenza F (1995) Effects of positive end-expiratory pressure on regional distribution of tidal volume and recruitment in adult respiratory distress syndrome. Am J Respir Crit Care Med 151: 1807–1814

3. Puybasset L, Cluzel P, Chao N, Slutsky A, Coriat P, Rouby JJ, CT Scan ARDS Study group (1998) A computed tomography assessment of regional lung volume in acute lung injury. Am J Respir Crit Care Med 158: 1644–1655

4. Gattinoni L, Pelosi P, Suter PM, Pedoto A, Vercesi P, Lissoni A (1998) Acute respiratory distress syndrome caused by pulmonary and extrapulmonary disease. Am J Respir Crit Care Med 158: 3–11
5. Puybasset L, Cluzel P, Gusman P, Grenier P, Preteux F, Rouby J-J, CT scan ARDS study group (2000) Regional distribution of gas and tissue in acute respiratory distress syndrome. I Consequences for lung morphology. Intensive Care Med 26: 857–869
6. Rouby J-J, Puybasset L, Cluzel P, Richecoeur J, Lu Q, Coriat P, CT scan ARDS study group (2000) Regional distribution of gas and tissue in acute respiratory distress syndrome. II. Physiological correlations and definition of an ARDS Severity Score. Intensive Care Med 26: 1046–1056
7. Vieira S, Puybasset L, Richecoeur J, Lu Q, Cluzel P, Gusman P, Coriat P, Rouby JJ (1998) A lung computed tomographic assessment of positive end-expiratory pressure-induced lung overdistension. Am J Respir Crit Care Med 158: 1571–1577
8. Gattinoni L, Pesenti A, Bombino M, Baglioni S, Rivolta M, Rossi G, Rossi F, Marcolin R, Mascheroni D, Torresin A (1988) Relationships between lung computer tomographic density, gas exchange, and PEEP in acute respiratory failure. Anesthesiology 69: 824–832
9. Vieira S, Puybasset L, Lu Q, Richecoeur J, Cluzel P, Coriat P, Rouby JJ (1999) A scanographic assessment of pulmonary morphology in acute lung injury: signification of the lower inflection point detected on the lung pressure-volume curve. Am J Respir Crit Care Med 159: 1612–1623
10. Gattinoni L, Mascheroni D, Torresin A, Marcolin R, Fumagalli R, Vesconi S, Rossi G, Rossi F, Baglioni S, Bassi F, Nastri F, Pesenti A (1986) Morphological response to positive end expiratory pressure in acute respiratory failure. Computerized tomography study. Intensive Care Med 12: 137–142
11. Gattinoni L, Pesenti A, Avalli L, Rossi F, Bombino M (1987) Pressure-volume curve of total respiratory system in acute respiratory failure. Computed tomographic scan study. Am Rev Respir Dis 136: 730–736
12. Gevenois PA, Vuyst P, Maertelaer V, Zanen J, Jacobovitz D, Cosio MG, Yernauld JC (1996) Comparison of computed density and microscopic morphometry in pulmonary emphysema. Am J Respir Crit Care Med 154: 187–192
13. Gould GA, Macnee W, Mclean A, Warren PM, Redpath A, Best JJK, Lamb D, Flenley DC (1988) CT measurements of lung density in life can quantitate distal airspace enlargement – An essential defining feature of human enphysema. Am Rev Respir Dis 137: 380–392
14. Hayhurst MD, Flenley DC, McLean A, Wightman AJA, MacNee W, Wright D, Lamb D, Best J (1984) Diagnosis of pulmonary emphysema by computerized tomography. Lancet II:320–322
15. Kinsella M, Müller NL, Abboud RT, Morreison NJ, DyBuncio A (1990) Quantitation of emphysema by computed tomography using a density mask program and correlation with pulmonary function tests. Chest 97: 315–321
16. Webb HH, Tierney DF (1974) Experimental pulmonary edema due to intermittent positive pressure ventilation with high inflation pressures. Protection by positive end- expiratory pressure. Am Rev Respir Dis 110: 556–565
17. Corbridge TC, Wood LD, Crawford GP, Chudoba MJ, Yanos J, Sznajder JI (1990) Adverse effects of large tidal volume and low PEEP in canine acid aspiration. Am Rev Respir Dis 142: 311–315
18. Dreyfuss D, Soler P, Basset G, Saumon G (1988) High inflation pressure pulmonary edema. Respective effects of high airway pressure, high tidal volume, and positive end-expiratory pressure. Am Rev Respir Dis 137: 1159–1164
19. Demling RH, Staub NC, Edmunds LH Jr (1975) Effect of end-expiratory airway pressure on accumulation of extravascular lung water. J Appl Physiol 38: 907–912
20. Malo J, Ali J, Wood LD (1984) How does positive end-expiratory pressure reduce intrapulmonary shunt in canine pulmonary edema? J Appl Physiol 57: 1002–1010
21. Greaves IA, Hildebrandt J, Hoppin FG (1986) Micromechanics of the lung. In: Macklem PT, Mead J (ed) Handbook of physiology. American Physiological Society, Bethesda
22. Ranieri VM, Eissa NT, Corbeil C, Chassé M, Braidy J, Matar N, Milic-Emili J (1991) Effects of positive end-expiratory presure on alveolar recruitment and gas exchange in patients with the Adult respiratory distress syndrome. Am Rev Respir Dis 144: 544–551
23. Jonson B, Richard JC, Straus C, Mancebo J, Lemaire F, Brochard L (1999) Pressure-volume curves and compliance in acute lung injury. Am J Respir Crit Care Med 159: 1172–1178
24. Roupie E, Dambrosio M, Servillo G, Mentec H, El Atrous S, Beydon L, Brun-Buisson C, Lemaire F, Brochard L (1995) Titration of tidal volume and induced hypercapnia in acute respiratory distress syndrome. Am J Respir Crit Care Med 152: 121–128